# Precision measurement of the light shift of $^{25}Mg^{+}$ ions

W. H. Yuan, K. Deng,* Z. Y. Ma, H. Che, Z. T. Xu, H. L. Liu, J. Zhang, and Z. H. Lu†
*MOE Key Laboratory of Fundamental Physical Quantities Measurements, Hubei Key Laboratory of Gravitation and Quantum Physics, School of Physics, Huazhong University of Science and Technology, Wuhan 430074, China*

(Received 20 August 2018; published 15 November 2018)

We calculate the polarizabilities of the Zeeman sublevels of $^{25}Mg^{+}$ ion hyperfine ground states. To verify the calculation result, a single $^{25}Mg^{+}$ ion is trapped in a Paul trap and a microwave resonance measurement is carried out on the ground states with and without the light shift. A good agreement between the experimental result and the calculation result is obtained.

DOI: 10.1103/PhysRevA.98.052507

## I. INTRODUCTION

Light shift, which is also called ac Stark shift, is induced by external oscillating electric fields. The light shift for a specific atomic state can be treated as the interaction of a field-induced atomic dipole moment with the dipole-inducing field [1,2]. In some cold atomic physics experiments such as Sisyphus cooling [3,4] and optical-lattice traps [5,6], the light shift is purposely used to manipulate atoms. However, in many other high-precision measurement experiments such as atomic clocks [6–11], atomic magnetometers [12–14], and atomic interferometers [15–17], the light shift perturbs the measurement by introducing instability, therefore the light shift needs to be carefully measured and controlled. Precision measurement of light shift can be used to calculate the atomic polarizability. The knowledge of atomic polarizability has many applications. In particular, the blackbody radiation shift [18,19], which depends on the atomic polarizability, is one of the leading terms of inaccuracy in many primary atomic microwave clocks and optical clocks [6,7,9,20,21]. Due to its importance in atomic and optical physics, much effort has been taken to calculate and measure the light shift for atoms such as Cs [20] and Rb [21].

Cooled and trapped ions in Paul traps can be treated as ideal quantum systems for precision measurements due to long interaction times and small Doppler broadening effects. $^{25}Mg^{+}$ ion is a good candidate for precision measurement and is widely used in quantum optics experiments. Several transition frequencies of $^{25}Mg^{+}$ ion are of particular interest for astrophysics and searches for variations of fundamental constants such as fine-structure constant $\alpha$ [22–24]. For example, the $^{25}Mg^{+}$ ion $D_1$ and $D_2$ lines (fine-structure doublet) near 280 nm have prominent features in many astronomical spectra [22]. When cosmological redshift shifts the strong uv lines into the transparency range, it can be easily observed by ground-based telescopes. Currently the measurement accuracy of the fine-structure doublet is at the level of several MHz, limited by the light shift of the cooling laser [25,26].

As the nuclear spin of the $^{25}Mg^{+}$ ion is nonzero, the splitting of the hyperfine components of the $^{25}Mg^{+}$ ion ground state with a frequency $\nu_{HFS} = 1.789$ GHz can be chosen as potential microwave clock transition [27]. Its level structure allows cooling, optical pumping, and interrogation with a single laser. Therefore it is a potential next-generation laser-cooled microwave atomic clock that can be used for space applications. To improve the performance of the clock, the light shift and the blackbody radiation shift need to be precisely evaluated.

In addition, $^{25}Mg^{+}$ ion is used for sympathetic cooling and quantum logic detection [10,28] in the $^{27}Al^{+}$ ion optical clock, which has very low sensitivity to electromagnetic perturbations and a narrow natural linewidth of 8 mHz. The $^{27}Al^{+}$ ion optical clock has reached the $10^{-18}$ systematic uncertainty level and is one of the most accurate optical clocks. The $^{25}Mg^{+}$ ion is a suitable ion for sympathetic cooling of the $^{27}Al^{+}$ ion since its mass is very close to that of the $^{27}Al^{+}$ ion. This ensures a very efficient energy transfer between these two ions. To implement quantum logic spectroscopy, the two hyperfine components of the ground state of the $^{25}Mg^{+}$ ion, $^2S_{1/2}|F = 3, m_F = 3\rangle$ (in the following, it will be written as $^2S_{1/2}|3, 3\rangle$ for simplicity) and $^2S_{1/2}|2, 2\rangle$, are treated as two spin levels of a quantum qubit. Raman sideband cooling is implemented for quantum logic spectroscopy and a Raman transition between $^2S_{1/2}|3, 2\rangle$ and $^2S_{1/2}|2, 2\rangle$ is used for repumping. In these situations the light shift of the two hyperfine ground states has significant effect on the signal-to-noise ratio of the quantum logic spectroscopy and needs to be precisely measured.

In this paper, we derive the polarizabilities of the Zeeman sublevels of the $^{25}Mg^{+}$ ion ground states and calculate the light shift when the laser intensity is equal to the saturation intensity. It is noted that using the same method that has been used with most other references [7,9,29–31], the form of expression of our calculation result differs with them on the vector polarizability while the expressions for the Stark shifts are the same. This is due to differences in the definition of polarizability $\alpha$. In this paper we use the definition in Ref. [1]. To verify our calculation result, we measure the light intensity of a circular polarized laser and the associated light shift. The light intensity is measured using a fluorescence fitting

*ke.deng@hust.edu.cn
†zehuanglu@hust.edu.cn

 

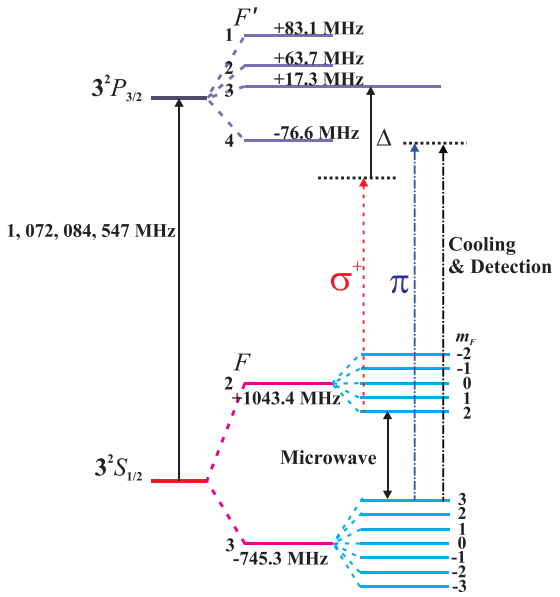


FIG. 1. The relevant energy levels of the $^{25}Mg^+$ ion. The cooling and detection laser is near resonant with the $^2S_{1/2}|3,3\rangle \rightarrow {}^2P_{3/2}|4,4\rangle$ cycling transition, the $\pi$ laser has the same frequency as that of the cooling laser, $\sigma^+$ is the laser for inducing the light shift, and $\Delta$ is the detuning of the $\sigma^+$ laser. The frequency of the microwave is about 1.79 GHz.

method. The light shift is measured using the microwave resonance method. The light shift of several Zeeman sublevels of the $^{25}Mg^+$ ion ground states are measured. In addition, the light shifts for the $^2S_{1/2}|3,3\rangle$ to $^2S_{1/2}|2,2\rangle$ transition under different laser detunings are also measured. All of the experimental results are consistent with our calculations.

The paper has four sections after the Introduction. Section II presents the basic theory and calculation results for the light shift of the $^{25}Mg^+$ ion ground states. Section III presents the experimental setup on the measurement of the light shift of the $^{25}Mg^+$ ion ground states in a linear Paul trap and the experimental procedures. Section IV provides the measurement results and comparison between the theory and experiment. The last section provides a brief summary.

## II. BASIC THEORY OF LIGHT SHIFT FOR $^{25}Mg^+$ ION

Figure 1 shows the relevant energy levels of the $D_2$ line of the $^{25}Mg^+$ ion and the microwave transitions between the ground-state hyperfine structures in the presence of magnetic field. The frequency of the ground-state hyperfine splitting is about 1.79 GHz. When a laser interrogates the ion, the energy of the microwave transition becomes

$$E = E_{\rm hfs} + \Delta E_{\rm Zeeman} + \Delta E^{\rm ac}. \tag{1}$$

Here $E_{\rm hfs} = \frac{1}{2}hA[F(F+1) - I(I+1) - J(J+1)]$ is the hyperfine-structure splitting, $h$ is the Planck's constant, $A$ is the magnetic dipole hyperfine coupling constant, $F$ is the total angular momentum, $I$ is the nuclear spin, and $J$ is the electron angular momentum. $\Delta E_{\rm Zeeman} = \mu_B g_F m_F B$ is the first-order Zeeman shift, where $\mu_B$ is the Bohr magneton, $g_F$ is the Landé $g$ factor, $m_F$ is the projection of $F$ on the quantization axis, and $B$ is the magnetic field that defines the quantization axis, which is taken along the $z$ axis. The first-order Zeeman shift for the $^2S_{1/2}|2,2\rangle$ state under 1-Gauss magnetic field is about 0.93 MHz. $\Delta E^{\rm ac}$ is the light shift caused by the laser field, and can be expressed as [9]

$$\Delta E^{\rm ac}(F, m_F; \omega) = -\alpha_{F,m_F}(\omega)\left(\frac{\epsilon}{2}\right)^2. \tag{2}$$

Here $\alpha_{F,m_F}$ is the polarizability of the $|F, m_F\rangle$ state, and $\epsilon$ and $\omega$ are the amplitude and angular frequency of the incident laser field. $\epsilon$ can be obtained from laser intensity, $I = \epsilon^2 n/(2\mu_0 c)$, where the refractive index in vacuum is $n = 1$, $\mu_0 = 4\pi \times 10^{-7}$ T m/A is the vacuum permeability, $c = 299\ 792\ 458$ m/s is the speed of light in vacuum. The light shift can be expanded by $m_F$ as [1]

$$\begin{aligned}\Delta E^{\rm ac}(F, m_F; \omega) &= -\alpha_F^S(\omega)|E_0^{(+)}|^2 - \alpha_F^V(\omega)(i\boldsymbol{E}_0^{(-)} \times \boldsymbol{E}_0^{(+)})_z \frac{m_F}{F} \\ &\quad - \alpha_F^T(\omega)\left(\frac{3|E_{0z}^{(+)}|^2 - |E_0^{(+)}|^2}{2}\right)\left[\frac{3m_F^2 - F(F+1)}{F(2F-1)}\right].\end{aligned} \tag{3}$$

Here $E_0^{(+)}$ and $E_0^{(-)}$ are the positive- and negative-frequency components of the laser field. $E_0^{(+)} = \epsilon$. $(i\boldsymbol{E}_0^{(-)} \times \boldsymbol{E}_0^{(+)})_z = |E_{0,-1}^{(+)}|^2 - |E_{0,1}^{(+)}|^2$, where $E_{0,\pm1}^{(+)}$ is the amplitude of $\sigma^\mp$ light. $E_{0z}^{(+)}$ is the laser field projection on the quantization axis. $\alpha_F^S(\omega)$, $\alpha_F^V(\omega)$, and $\alpha_F^T(\omega)$ are atomic scalar, vector, and tensor polarizabilities, and are defined as [1]

$$\alpha_F^S(\omega) = \sum_{F'} \frac{2\omega_{F'F}|\langle F||d||F'\rangle|^2}{3\hbar({\omega_{F'F}}^2 - \omega^2)}, \tag{4}$$

$$\begin{aligned}\alpha_F^V(\omega) &= \sum_{F'}(-1)^{F+F'+1}\sqrt{\frac{6F(2F+1)}{F+1}} \\ &\quad \times \begin{Bmatrix} 1 & 1 & 1 \\ F & F & F' \end{Bmatrix} \frac{\omega_{F'F}|\langle F||d||F'\rangle|^2}{\hbar({\omega_{F'F}}^2 - \omega^2)},\end{aligned} \tag{5}$$

$$\begin{aligned}\alpha_F^T(\omega) &= \sum_{F'}(-1)^{F+F'}\sqrt{\frac{40F(2F+1)(2F-1)}{3(F+1)(2F+3)}} \\ &\quad \times \begin{Bmatrix} 1 & 1 & 2 \\ F & F & F' \end{Bmatrix} \frac{\omega_{F'F}|\langle F||d||F'\rangle|^2}{\hbar({\omega_{F'F}}^2 - \omega^2)},\end{aligned} \tag{6}$$

where $\omega_{F'F}$ is the unperturbed $D_2$ line resonant transition frequency. For the hyperfine ground state $|F=2\rangle$, three $|F=2\rangle \rightarrow |F'=1,2,3\rangle$ transitions are considered. For the hyperfine ground state $|F=3\rangle$, another $|F=3\rangle \rightarrow |F'=2,3,4\rangle$ transitions are considered. $\omega$ is the frequency of the laser which is used to induce the light shift. $\{{}^1_F\ {}^1_F\ {}^1_{F'}\}$ and $\{{}^1_F\ {}^1_F\ {}^2_{F'}\}$ are the Wiger 6-$j$ symbols. $\langle F||d||F'\rangle$ is the reduced matrix element of the electric dipole moment, and can be further written as

$$\begin{aligned}|\langle F||d||F'\rangle| &= (-1)^{J+I+F'+1}\sqrt{(2F'+1)(2J+1)} \\ &\quad \times \begin{Bmatrix} J & J' & 1 \\ F' & F & I \end{Bmatrix} |\langle J||d||J'\rangle|.\end{aligned} \tag{7}$$

TABLE I. The scalar, vector, and tensor polarizabilities of the $^{25}Mg^{+}$ ion hyperfine ground states $|F=2\rangle$ and $|F=3\rangle$ when the $\sigma^{+}$ laser has a red detuning of 9.2 GHz.

| Term | Dynamic polarizability in $J/(V/m)^2 \times 10^{-35}$ |
|---|---|
| $\alpha_2^S(\omega)$ | 2.19 |
| $\alpha_3^S(\omega)$ | 1.86 |
| $\alpha_2^V(\omega)$ | −0.73 |
| $\alpha_3^V(\omega)$ | 0.94 |
| $\alpha_2^T(\omega)$ | 0.0004 |
| $\alpha_3^T(\omega)$ | −0.0036 |

Here $|\langle J||d||J'\rangle| = \sqrt{\frac{3\varepsilon_0 hc^3}{2\tau\omega^3}\times\frac{2J'+1}{2J+1}}$ [32]. $\varepsilon_0$ is the vacuum permittivity, $\tau = 3.810(40)$ ns [33], $\omega = 2\pi\times 1072\,085$ GHz [34]. So $|\langle J||d||J'\rangle| = |\langle 1/2||d||3/2\rangle| = 2.018\times 10^{-29}$ C m. In the experiment, the laser for light-shift measurement is a $\sigma^{+}$ laser propagating along the magnetic field direction, so Eq. (3) becomes

$$E^{\rm ac}(F,m_F;\omega) = -\left\{\alpha_F^S(\omega)+\frac{m_F}{F}\alpha_F^V(\omega) - \frac{3m_F^2-F(F+1)}{2F(2F-1)}\alpha_F^T(\omega)\right\}\left(\frac{\epsilon}{2}\right)^2. \quad (8)$$

Our experimental results agree with Eq. (8).

The frequency of the $\sigma^{+}$ laser is red-detuned from the $^2S_{1/2}|3,3\rangle \rightarrow {}^2P_{3/2}|4,4\rangle$ cycling transition for several GHz to tens of GHz. We can calculate the dynamic polarizabilities for the two hyperfine ground states under this laser interaction. For a laser detuning of 9.2 GHz the results are shown in Table I.

From the light shift of each Zeeman sublevel we can obtain the light shift of a specified microwave transition between $^2S_{1/2}|2,m_1\rangle$ and $^2S_{1/2}|3,m_2\rangle$ to be

$$\Delta\omega_{\rm LS} = \frac{\alpha_{2,m_1}(\omega)-\alpha_{3,m_2}(\omega)}{\hbar}\left(\frac{\epsilon}{2}\right)^2. \quad (9)$$

## III. EXPERIMENTAL SETUP AND PROCEDURES

### A. Experimental setup

The experimental setup is shown in Fig. 2. A linear Paul trap [35–37] is used to trap a single $^{25}Mg^{+}$ ion in the experiment. The linear Paul trap consists of four blade-shaped electrodes and two end-cap electrodes. A pair of opposing blade-shaped electrodes is fed with a high voltage RF power and the other pair is grounded. The blade-shaped electrodes supply the radial confinement for ions. The high voltage RF power with a frequency of 24 MHz is first produced by a frequency synthesizer, and is amplified by an RF amplifier followed by a homemade helical resonator [38]. The distance between the two opposing blade-shaped electrodes is $2r = 1.6$ mm, and between the two end caps is $2z = 4.0$ mm; dc voltages are applied to the end-cap electrodes to confine ions axially. A quarter-wave antenna made with aluminum is installed inside the vacuum chamber. The antenna is designed with a resonance frequency of 1.79 GHz, which is roughly the

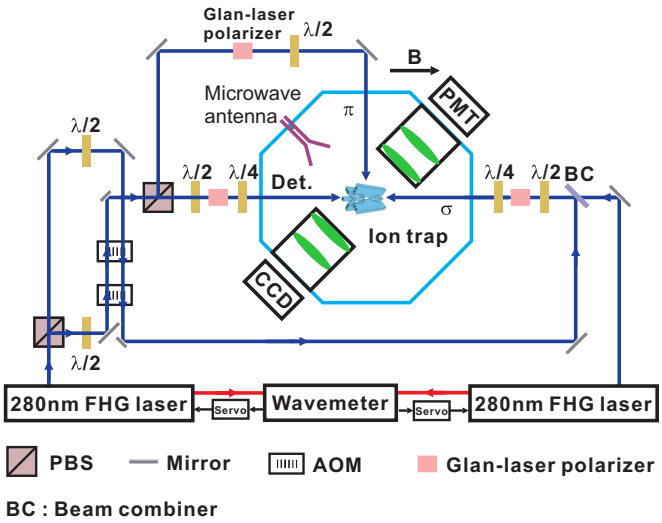


FIG. 2. Schematic of the experimental setup. The detection laser beam counterpropagates with the $\sigma^{+}$ laser which generates the light shift. A linearly polarized $\pi$ beam propagates perpendicularly for state preparation. CCD and PMT are used to detect the fluorescence signal of the ions.

frequency difference of the ground-state hyperfine splitting of the $^{25}Mg^{+}$ ion. The pressure in the vacuum chamber is about $5\times 10^{-9}$ Pa.

$^{25}Mg^{+}$ ions are loaded by laser ablation. A Mg wire with a diameter of 0.5 mm is installed near the trap as the Mg target. For laser ablation a frequency-doubled Nd:YAG laser at 532 nm with a pulse duration of 2 ns and a maximum pulse energy of 150 $\mu$J is used. To improve the loading efficiency, a frequency-quadrupled 285-nm laser is used for photoionization. A frequency-quadrupled 280-nm laser is used to cool and detect $^{25}Mg^{+}$ ions [39]. Another frequency-quadrupled 280-nm laser is used to induce light shift while its frequency has variable detunings with respect to the $^2S_{1/2}|3,3\rangle \rightarrow {}^2P_{3/2}|4,4\rangle$ cycling transition.

Three pairs of Helmholtz coils are mounted around the vacuum chamber to compensate stray magnetic field and supply the quantization axis. The magnetic field is in the direction of the Doppler cooling beam to allow driving of the cycling transition with circularly polarized light. The magnetic field direction has an angle of 45 degrees with respect to the trap axis. Normally a 6-Gauss magnetic field is used in the experiment, generating a frequency difference of about 2.8 MHz between adjacent Zeeman sublevels. To obtain the circularly polarized beam, we use a Glan laser polarizer and a half-wave plate to obtain the linearly polarized beam, and then use a quarter-wave plate to obtain the circularly polarized beam. All beams are focused onto the center of the trap region to achieve high enough light intensity. The $\sigma^{+}$ laser which causes the light shift counterpropagates with the cooling laser. Two fused silica re-entrant viewports are installed on the vacuum chamber to collect the fluorescence of the ions. The fluorescence collection efficiency is about 0.4%.

### B. Experimental procedures

When a single Mg ion is loaded in the trap, it is Doppler cooled first. For Doppler cooling, the cooling laser is

red-detuned by half the linewidth with respect to the cycling transition from $^2S_{1/2}|3,3\rangle$ to $^2P_{3/2}|4,4\rangle$. In order to compare with the calculated light shift we shall first measure the light intensity. A straightforward method to measure the intensity is to measure the laser beam power and the laser beam size. In our system the beam is focused to the trap center by a lens with a focal length of 200 mm. The lens is outside the vacuum chamber. The waist diameter is about 48 $\mu$m. If we reflect the beam outside the vacuum chamber and measure its focused spot area, a 2- to 3-mm distance uncertainty along the beam path will cause a 11%–25% error of the focused spot area, while our razor blade setup for measuring the beam diameter also introduces extra errors due to insufficient step resolution. So the potential error could be quite large using this direct method. As a matter of fact there is a 25% discrepancy between this direct method result and the fluorescence-fitting method result. We judge that the fluorescence-fitting method will be more accurate since it can give the light intensity that an ion actually feels. The basic idea of the fluorescence-fitting method is to measure the saturation parameter $S$ of the laser light and then use the expression $I = SI_S$, where $I$ is the incident laser intensity and $I_S$ is the saturation intensity. For the cycling transition the saturation intensity can be calculated as $I_S = \hbar\omega^3\Gamma/(12\pi c^2) \approx 2470\,\mathrm{W/m^2}$. Here $\Gamma$ is the $^{25}Mg^+$ ion spontaneous emission rate, $\Gamma = 41.7$ MHz, $\omega = 1072.1$ THz is the transition frequency of the $D_2$ line as shown in Fig. 1. $S$ can be obtained based on $S = P/P_S$. $P$ and $P_S$ are the laser power corresponding to $I$ and $I_S$. $P$ can be measured by a power meter. $P_S$ can be obtained by fitting the fluorescence rate of a single ion as a function of laser power $P$. The collected fluorescence rate $F(P)$ of a single ion as a function of detection laser power $P$ can be expressed as [32]

$$F(P) = \frac{\eta\Gamma}{2\left[1+\left(1+\frac{4\Delta_D^2}{\Gamma^2}\right)\frac{P_S}{P}\right]}. \tag{10}$$

Here $\eta$ is the fluorescence collection efficiency, and $\Delta_D$ is the frequency detuning of the detection laser from the cycling transition. This method requires the laser beam to have perfect circular polarization to drive the cycling transition, and is frequency stabilized.

To measure the light shift, we measure the transition frequency of different Zeeman sublevels of the hyperfine ground states by a microwave resonance method with and without light shift. For the microwave resonance method, the ion is first prepared in the $^2S_{1/2}|3,3\rangle$ state by applying the Doppler cooling and repumping beams for 0.3 ms, followed by a $\pi$ polarized light. The intensity of the $\pi$ laser is about 10 times saturation intensity. All five Zeeman sublevels of the ground $|F=2\rangle$ state can be populated, but the relative population depends on the applied $\pi$ light pulse time. For different Zeeman sublevels the needed $\pi$ light pulse time is different. For example, for pumping $|3,3\rangle$ to $|2,2\rangle$ the pulse time is about several $\mu$s, and $|3,3\rangle$ to $|2,-2\rangle$ pumping takes over 100 $\mu$s since more transitions are needed. Then it interacts with a microwave pulse. After the microwave pulse interrogation, the ion will fall to a superposition state of the $|F=2\rangle$ state and the $|F=3\rangle$ state. After that, state detection is achieved by applying the resonant Doppler cooling beam and counting the number of detected photons. The resonant Doppler cooling laser drives the $^2S_{1/2}|3,3\rangle$ to $^2P_{3/2}|4,4\rangle$ cycling transition. All the $|F=3\rangle$ states are bright states, which will produce a mean photon number of 12 with 50-$\mu$s detection time. All the $|F=2\rangle$ states are dark states, under which the mean photon number is about 1 with the same detection time of 50 $\mu$s.

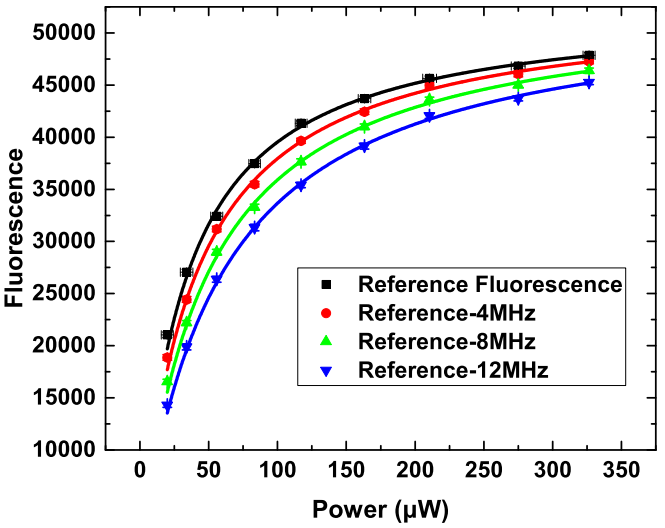


FIG. 3. Fluorescence per 0.1 second vs laser power at different frequency detunings $\Delta_D$ of the detection laser. For the reference fluorescence curve, the frequency detuning $\Delta_D$ is 8(1) MHz. For the other three plotted curves, they have additional 4-, 8-, and 12-MHz red detuning compared to the reference.

The resonant frequency $\omega_0$ is measured again while the $\sigma^+$ laser light irradiates the ion during the microwave pulse interrogation. The measured $\omega_0$ will be shifted by the $\sigma^+$ laser light. From the measured frequency difference we can obtain the light shift.

From Eq. (8), it can be seen that $m_F$ affects the polarizability significantly. To confirm Eq. (8), we measure the light shift for different Zeeman sublevels. In the experiment

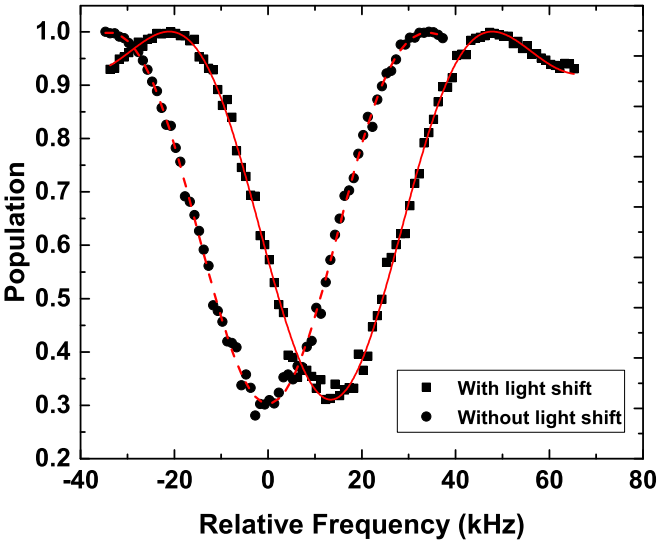


FIG. 4. Typical microwave resonance spectrum of the $|2,2\rangle$ to $|3,3\rangle$ transition with and without the light shift.

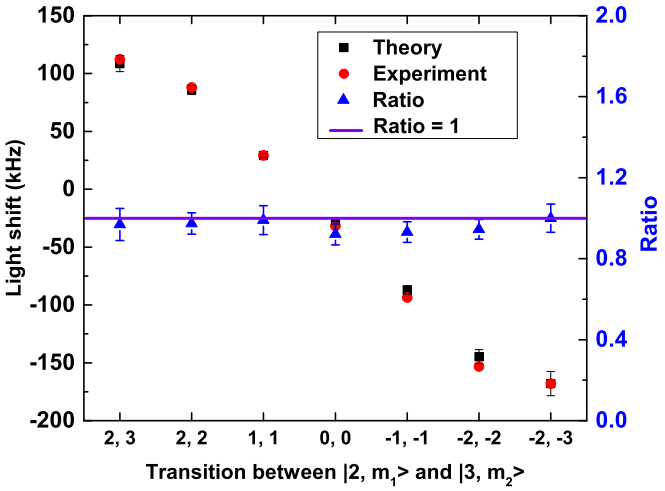


FIG. 5. The light shifts for the seven microwave transitions. Black squares, theoretical results; red circles, experimental results; blue triangles, the ratio of theoretical and experimental results. The purple line corresponds to a ratio of one.

we measured frequencies with and without the light shift for seven microwave transitions in the ground Zeeman sublevels. They are ${}^2S_{1/2}|2,2\rangle \rightarrow {}^2S_{1/2}|3,3\rangle$, ${}^2S_{1/2}|2,2\rangle \rightarrow {}^2S_{1/2}|3,2\rangle$, ${}^2S_{1/2}|2,1\rangle \rightarrow {}^2S_{1/2}|3,1\rangle$, ${}^2S_{1/2}|2,0\rangle \rightarrow {}^2S_{1/2}|3,0\rangle$, ${}^2S_{1/2}|2,-1\rangle \rightarrow {}^2S_{1/2}|3,-1\rangle$, ${}^2S_{1/2}|2,-2\rangle \rightarrow {}^2S_{1/2}|3,-2\rangle$, and ${}^2S_{1/2}|2,-2\rangle \rightarrow {}^2S_{1/2}|3,-3\rangle$. Some symmetric transitions are not included because they have the same resonant frequencies if the Zeeman effect is taken into account. For example, both the ${}^2S_{1/2}|2,2\rangle \rightarrow {}^2S_{1/2}|3,1\rangle$ transition and the ${}^2S_{1/2}|2,1\rangle \rightarrow {}^2S_{1/2}|3,2\rangle$ transition have the resonant frequency of $(E_{\rm hfs} - 3\mu_B g_F B)/\hbar = (E_{\rm hfs} - \mu_B B)/\hbar$.

## IV. EXPERIMENTAL RESULTS

From Eq. (10), the laser detuning $\Delta_D$ can affect the fitting result of the saturation parameter, so we fix the detuning of the detection laser before curve fitting. A precise method to obtain the detuning is to scan the complete Voigt profile of the fluorescence spectrum. However, after the laser is blue-detuned, the ion will be heated and the fluorescence signal drops quickly to zero. Therefore we use a simpler method that still ensures enough accuracy. First we cool the ion to the Doppler limit, then we scan half of the Voigt profile to get a rough estimation of the resonant frequency, which has an error about 2 MHz. To reduce the error, we measured several curves of $F(P)$ as a function of $P$ under different laser detunings $\Delta_D$, as shown in Fig. 3. In our experiment, the reference frequency has a red detuning of 8(1) MHz. From the fitting of these curves, we can obtain the saturation power $P_S$ for the $\sigma^+$ laser to be 29.7(1.2) $\mu$W.

Based on the microwave resonance method, resonant frequency of the ground-state sublevels can be measured. Figure 4 shows a typical Rabi spectrum of the microwave transition. The center frequency is obtained by fitting from the curves. From the two curves in Fig. 4 the light shift can be obtained. The error for measuring the resonant frequency is mainly caused by the residual magnetic field fluctuation (about several mG) and the long-term laser intensity drift (about 3.5%). The magnetic field fluctuation can affect the light shift measurement by several kHz. To reduce the influence of the magnetic field fluctuation, the saturation parameter of the $\sigma^+$ laser is set at more than 10 to induce a relatively large light shift.

The experimental results on seven Zeeman sublevel transitions are shown in Fig. 5 and Table II. The theoretical values based on our calculations are also shown. Here the theoretical light shift is derived by using the measured light intensity and the calculated dynamical polarizabilities. From the results it can be seen that the experimental results agree with theory very well. We also give the relative contributions of the three Stark shifts as shown in Table III. It can be seen that both scalar and vector terms have large contributions. The tensor terms are very small and can be neglected. Our measurements are sensitive to the scalar and vector terms. If the vector part has a coefficient of $m_F/2F$ instead of $m_F/F$, it would have a strong impact on the agreement between the theory and the experimental results. We can use the data to extract experimental values of

TABLE III. The relative contributions of the three Stark shifts.

| $\lvert F=2,m_1\rangle \rightarrow \lvert F=3,m_2\rangle$ | Scalar (kHz) | Vector (kHz) | Tensor (kHz) |
|---|---|---|---|
| $\lvert 2,2\rangle \rightarrow \lvert 3,3\rangle$ | −26.7(1.9) | 135.9(9.4) | 0.02(0) |
| $\lvert 2,2\rangle \rightarrow \lvert 3,2\rangle$ | −27.8(1.4) | 114.3(5.7) | 0.02(0) |
| $\lvert 2,1\rangle \rightarrow \lvert 3,1\rangle$ | −28.5(1.2) | 58.6(2.4) | −0.10(0) |
| $\lvert 2,0\rangle \rightarrow \lvert 3,0\rangle$ | −28.0(1.2) | 0 | −0.14(1) |
| $\lvert 2,-1\rangle \rightarrow \lvert 3,-1\rangle$ | −28.0(1.2) | −57.6(2.4) | −0.10(0) |
| $\lvert 2,-2\rangle \rightarrow \lvert 3,-2\rangle$ | −28.0(1.2) | −115.2(4.8) | 0.02(0) |
| $\lvert 2,-2\rangle \rightarrow \lvert 3,-3\rangle$ | −27.6(1.6) | −139.5(8.2) | 0.17(1) |

TABLE II. The experimental and theoretical results of the relevant seven microwave transitions.

| $\lvert F=2,m_1\rangle \rightarrow \lvert F=3,m_2\rangle$ | Measured light shift (kHz) | Saturation parameter $S$ | Theoretical light shift (kHz) |
|---|---|---|---|
| $\lvert 2,2\rangle \rightarrow \lvert 3,3\rangle$ | 112.2(1.9) | 11.6(0.8) | 112.0(7.4) |
| $\lvert 2,2\rangle \rightarrow \lvert 3,2\rangle$ | 88.1(0.7) | 12.0(0.6) | 88.5(4.2) |
| $\lvert 2,1\rangle \rightarrow \lvert 3,1\rangle$ | 29.4(0.8) | 12.3(0.5) | 30.0(1.3) |
| $\lvert 2,0\rangle \rightarrow \lvert 3,0\rangle$ | −31.7(0.5) | 12.1(0.5) | −30.1(1.3) |
| $\lvert 2,-1\rangle \rightarrow \lvert 3,-1\rangle$ | −93.4(1.1) | 12.1(0.5) | −89.7(3.9) |
| $\lvert 2,-2\rangle \rightarrow \lvert 3,-2\rangle$ | −153.1(1.4) | 12.1(0.5) | −144.7(7.4) |
| $\lvert 2,-2\rangle \rightarrow \lvert 3,-3\rangle$ | −168.0(1.2) | 11.9(0.7) | −173.1(11.1) |

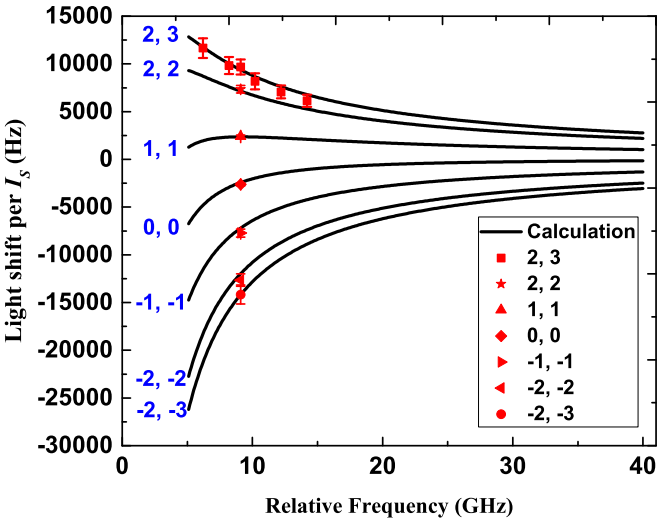


FIG. 6. The black curves are the theoretical light shifts under saturated intensity $I_S$ at different dutuning frequencies of the $\sigma^+$ light. The relative frequency is relative to the transition of $|F = 3\rangle$ to the excited state $|F = 4\rangle$. The red data points are our experimental results.

$\alpha_2^S - \alpha_3^S$, $\alpha_2^V$, and $\alpha_3^V$. The results are $\alpha_2^S - \alpha_3^S = 0.36(3) \times 10^{-35}\,\mathrm{J/(V/m)^2}$, $\alpha_2^V = -0.90(16) \times 10^{-35}\,\mathrm{J/(V/m)^2}$, $\alpha_3^V = 0.80(23) \times 10^{-35}\,\mathrm{J/(V/m)^2}$. These three values agree with the calculated values in Table I within the uncertainty range. The two scalar polarizabilities cannot be individually extracted because in the measured seven transitions the coefficients of the two terms are linearly dependent.

To study the relation of the laser frequency $\omega$ and the polarizability $\alpha$, we also measure the light shift for the transition $|2, 2\rangle \rightarrow |3, 3\rangle$ under different frequency detunings. The experimental results are shown in Fig. 6, and again agree with theory very well.

## V. CONCLUSION

In conclusion, we have calculated the frequency-dependent dynamical polarizabilities and differential light shifts of the $^{25}Mg^+$ ion hyperfine ground-state sublevels. To verify our calculations, we measured the differential light shifts of the $^{25}Mg^+$ ion ground-state Zeeman sublevels interacting with a $\sigma^+$ light using a microwave resonance method. The experimental results agree well with our calculated results.

## ACKNOWLEDGMENTS

The project is partially supported by the National Key R&D Program of China (Grant No. 2017YFA0304401) and the National Natural Science Foundation of China (Grants No. 11304109, No. 11174095, and No. 91336213).

[1] D. A. Steck, *Quantum and Atom Optics* (2016) available online at [http://www.steck.us/teaching] (revision No. 0.11.5; November 27, 2016).
[2] L. C. Biedenharn, G. A. Rinker, and J. C. Solem, J. Opt. Soc. Am. B **6**, 221 (1989).
[3] Claude N. Cohen-Tannoudji, Rev. Mod. Phys. **70**, 707 (1998).
[4] D. J. Wineland, J. Dalibard, and C. Cohen-Tannoudji, J. Opt. Soc. Am. B **9**, 32 (1992).
[5] T. Akatsuka, M. Takamoto, and H. Katori, Phys. Rev. A **81**, 023402 (2010).
[6] B. J. Bloom, T. L. Nicholson, J. R. Williams, S. L. Campbell, M. Bishof, W. Z. X. Zhang, S. L. Bromley, and J. Ye, Nature (London) **506**, 71 (2014).
[7] P. Rosenbusch, S. Ghezali, V. A. Dzuba, V. V. Flambaum, K. Beloy, and A. Derevianko, Phys. Rev. A **79**, 013404 (2009).
[8] B. Arora and B. K. Sahoo, Phys. Rev. A **86**, 033416 (2012).
[9] A. Derevianko and H. Katori, Rev. Mod. Phys. **83**, 331 (2011).
[10] C. W. Chou, D. B. Hume, J. C. J. Koelemeij, D. J. Wineland, and T. Rosenband, Phys. Rev. Lett. **104**, 070802 (2010).
[11] N. Nemitz, T. Ohkubo, M. Takamoto, I. Ushijima, M. Das, N. Ohmae, and H. Katori, Nature Photon. **10**, 258 (2016).
[12] J. C. Allred, R. N. Lyman, T. W. Kornack, and M. V. Romalis, Phys. Rev. Lett. **89**, 130801 (2002).
[13] I. K. Kominis, T. W. Kornack, J. C. Allred, and M. V. Romalis, Nature (London) **422**, 596 (2003).
[14] R. Dong, R. Wei, Y. Du, F. Zou, J. Lin, and Y. Wang, Appl. Phys. Lett. **106**, 152402 (2015).
[15] G. W. Biedermann, X. Wu, L. Deslauriers, S. Roy, C. Mahadeswaraswamy, and M. A. Kasevich, Phys. Rev. A **91**, 033629 (2015).
[16] R. Charrière, M. Cadoret, N. Zahzam, Y. Bidel, and A. Bresson, Phys. Rev. A **85**, 013639 (2012).
[17] B. Dubetsky and M. A. Kasevich, Phys. Rev. A **74**, 023615 (2006).
[18] T. Middelmann, S. Falke, C. Lisdat, and U. Sterr, Phys. Rev. Lett. **109**, 263004 (2012).
[19] S. G. Porsev and A. Derevianko, Phys. Rev. A **74**, 020502 (2006).
[20] K. Beloy, U. I. Safronova, and A. Derevianko, Phys. Rev. Lett. **97**, 040801 (2006).
[21] M. S. Safronova, D. Jiang, and U. I. Safronova, Phys. Rev. A **82**, 022510 (2010).
[22] M. Aldenius, S. Johansson, and M. T. Murphy, Monthly Notices of the Royal Astronomical Society **370**, 444 (2006).
[23] J. C. Berengut and V. V. Flambaum, Hyperfine Interact. **196**, 269 (2010).
[24] J. K. Webb, V. V. Flambaum, C. W. Churchill, M. J. Drinkwater, and J. D. Barrow, Phys. Rev. Lett. **82**, 884 (1999).
[25] M. Herrmann, V. Batteiger, S. Knünz, G. Saathoff, T. Udem, and T. W. Hänsch, Phys. Rev. Lett. **102**, 013006 (2009).
[26] V. Batteiger, S. Knünz, M. Herrmann, G. Saathoff, H. A. Schüssler, B. Bernhardt, T. Wilken, R. Holzwarth, T. W. Hänsch, and T. Udem, Phys. Rev. A **80**, 022503 (2009).
[27] I. V. Zalivako, I. A. Semerikov, A. S. Borisenko, K. Y. Khabarova, V. N. Sorokin, and N. N. Kolachevsky, Quantum Electron. **47**, 426 (2017).
[28] P. O. Schmidt, T. Rosenband, C. Langer, W. M. Itano, J. C. Bergquist, and D. J. Wineland, Science **309**, 749 (2005).

[29] Q.-Q. Hu, C. Freier, Y. Sun, B. Leykauf, V. Schkolnik, J. Yang, M. Krutzik, and A. Peters, Phys. Rev. A **97**, 013424 (2018).
[30] F. Le Kien, P. Schneeweiss, and A. Rauschenbeutel, Eur. Phys. J. D **67**, 92 (2013).
[31] R. Chicireanu, K. D. Nelson, S. Olmschenk, N. Lundblad, A. Derevianko, and J. V. Porto, Phys. Rev. Lett. **106**, 063002 (2011).
[32] R. Loudon, *The Quantum Theory of Light*, 3rd ed. (Oxford University Press, New York, 2000).
[33] W. Ansbacher, Y. Li, and E. H. Pinnington, Phys. Lett. A **139**, 165 (1989).
[34] G. Clos, M. Enderlein, U. Warring, T. Schaetz, and D. Leibfried, Phys. Rev. Lett. **112**, 113003 (2014).
[35] W. Paul, Rev. Mod. Phys. **62**, 531 (1990).
[36] H. Che, K. Deng, Z. T. Xu, W. H. Yuan, J. Zhang, and Z. H. Lu, Phys. Rev. A **96**, 013417 (2017).
[37] Z. T. Xu, K. Deng, H. Che, W. H. Yuan, J. Zhang, and Z. H. Lu, Phys. Rev. A **96**, 052507 (2017).
[38] K. Deng, Y. L. Sun, W. H. Yuan, Z. T. Xu, J. Zhang, Z. H. Lu, and J. Luo, Rev. Sci. Instrum. **85**, 104706 (2014).
[39] J. Zhang, W. H. Yuan, K. Deng, A. Deng, Z. T. Xu, C. B. Qin, Z. H. Lu, and J. Luo, Rev. Sci. Instrum. **84**, 123109 (2013).